

# Maximum Drag Reduction Asymptotes and the Cross-Over to the Newtonian Plug

By R. BENZI<sup>1</sup>, E. DE ANGELIS<sup>2</sup>, V. S. L'VOV<sup>3</sup>, I. PROCACCIA<sup>3</sup>  
and V. TIBERKEVICH<sup>3</sup>

<sup>1</sup> Dip. di Fisica and INFM, Università “Tor Vergata”, Via della Ricerca Scientifica 1, I-00133 Roma, Italy, <sup>2</sup> Dip. Mecc. Aeron., Università di Roma “La Sapienza”, Via Eudossiana 18, 00184, Roma, Italy, <sup>3</sup> Dept. of Chemical Physics, The Weizmann Institute of Science, Rehovot, 76100 Israel.

(Received 13 may 2004 and in revised form ??)

We employ the full FENE-P model of hydrodynamics of a dilute polymer solutions to derive a theoretical approach to drag reduction in wall bounded turbulence. We recapture the results of a recent simplified theory which derived the universal Maximum Drag Reduction (MDR) asymptote, and complement that theory with a discussion of the cross-over from the MDR to the Newtonian plug when the drag reduction saturates. The FENE-P model gives rise to a rather complex theory due to the interaction of the velocity field with the polymeric conformation tensor, making analytic estimates quite taxing. To overcome this we develop the theory in a computer-assisted manner, checking at each point the analytic estimates by Direct Numerical Simulations (DNS) of viscoelastic turbulence in a channel.

---

## 1. Introduction

The onset of turbulence in fluid flows is accompanied by a significant increase in the drag Lumley (1969), Sreenivasan & White (2000). This drag poses a real technological hindrance to the transport of fluids and to navigation of ships. It is interesting therefore that the addition of long chain polymers to wall-bounded turbulent flows can result in a significant reduction in the drag. The basic experimental knowledge of the phenomenon had been reviewed and systematized by Virk (1975); the amount of drag depends on the characteristics of the polymer and its concentration, but cannot exceed a universal asymptote known as the “Maximum Drag Reduction” (MDR) curve which is independent of the polymer’s concentration or its characteristics. When the concentration is not large enough, the mean velocity profile as a function of the distance from the wall follows the MDR for a while and then crosses back to a Newtonian-like profile, cf. Fig. 1 left.

Recently the nature of the MDR and the mechanism leading to its establishment were rationalized, using a phenomenological theory in which the role of the polymer conformation tensor was modeled by an effective viscosity L’vov et. al. (2003). It turned out that the effective viscosity attains a self-consistent profile, increasing linearly with the distance from the wall. With this profile the reduction in the momentum flux from the bulk to the wall overwhelms the increased dissipation that results from the increased viscosity. Thus the mean momentum increases in the bulk, and this is how drag reduction is realized. In De Angelis et. al. (2004) it was demonstrated by DNS that Navier-Stokes flows with viscosity profiles that vary linearly with the distance from the wall indeed

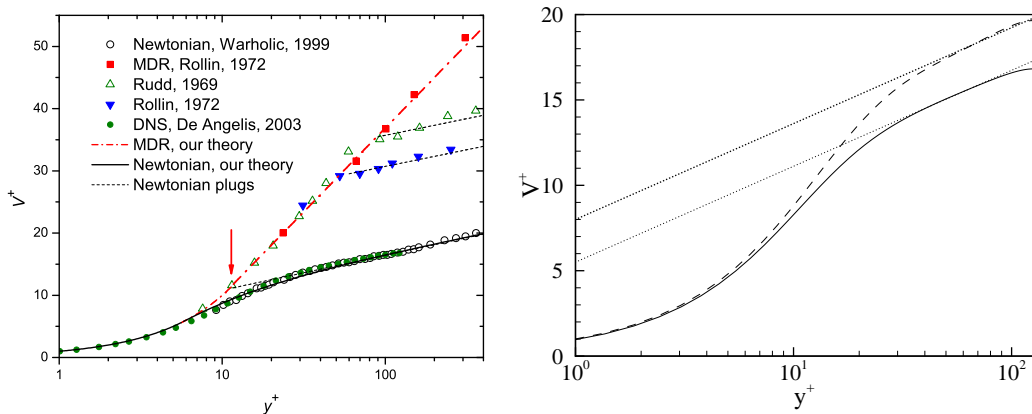


FIGURE 1. Left panel: Mean normalized velocity profiles as a function of the normalized distance from the wall during drag reduction. The data points from numerical simulations (green circles) and the experimental points (open circles) represent the Newtonian results. The red data points (squares) represent the Maximum Drag Reduction (MDR) asymptote. The dashed red curve represents the theory discussed in the paper which agrees with the universal MDR. The arrow marks the crossover from the viscous layer to the Newtonian log-law of the wall. The blue filled triangles and green open triangles represent the crossover, for intermediate concentrations of the polymer, from the MDR asymptote to the Newtonian plug. Right panel: Mean velocity profiles for the Newtonian and for the viscoelastic simulations with  $Re_\tau = 125$ . Solid line: Newtonian. Dashed line: Viscoelastic. The straight lines represent the classical von-Kármán log-law. The coordinate  $y^+$  is the distance from the wall in Pradtl units  $y^+ = v_* L / \nu$ , where  $v_*^2 = p' L$ .

show drag reduction in close correspondence with the phenomenon seen in full viscoelastic simulations. The aim of this paper is to complement the simplified theory with a derivation of the same results on the basis of a full viscoelastic model of the hydrodynamics of dilute polymer solutions. Such a derivation forsakes some of the simplicity of the phenomenological theory, but on the other hands it clarifies the role of the polymer conformation tensor in furnishing viscosity-like contributions. The relative complexity of the statistical theory is handled by employing suitable approximations for the leading terms and by computer assisted estimates of competing terms, allowing us at the end to provide a compact theory with sharp predictions. In addition to lending further support to the model of L'vov et. al. (2003), we will offer a discussion of the non-universal saturation of drag reduction as a function of concentration, length of polymer and relaxation time in various conditions of experimental interests.

In Sect. 2 we consider the FENE-P model of viscoelastic flows and review shortly the evidence for drag reduction in DNS of this model. In Sect. 3 we employ the FENE-P model to derive a statistical theory of drag reduction in wall bounded turbulence. In Sect. 4 we use the theory to predict the cross-over from the universal MDR to the Newtonian plug when the conditions differ from those necessary for attaining the MDR. In Sect. 5 we present a summary and a discussion.

## 2. Equations of motion for viscoelastic flows and drag reduction

Viscoelastic flows are represented well by hydrodynamic equations in which the effect of the polymer enters in the form of a “conformation tensor”  $R_{ij}(r, t)$  which stems from the ensemble average of the dyadic product of the end-to-end distance of the polymer chains Bird et. al. (1987), Beris & Edwards (1994). A successful model that had been

employed frequently in numerical simulations of turbulent channel flows is the FENE-P model Bird et. al. (1987). Flexibility and finite extensibility of the polymer chains are reflected by the relaxation time  $\tau$  and the Peterlin function  $P(r, t)$  which appear in the equation of motion for  $R_{ij}$ :

$$\frac{\partial R_{\alpha\beta}}{\partial t} + (u_\gamma \nabla_\gamma) R_{\alpha\beta} = \frac{\partial u_\alpha}{\partial r_\gamma} R_{\gamma\beta} + R_{\alpha\gamma} \frac{\partial u_\beta}{\partial r_\gamma} - \frac{1}{\tau} [P(r, t) R_{\alpha\beta} - \rho_0^2 \delta_{\alpha\beta}] , \quad (2.1)$$

$$P(r, t) = (\rho_m^2 - \rho_0^2) / (\rho_m^2 - R_{\gamma\gamma}) . \quad (2.2)$$

In these equations  $\rho_m^2$  and  $\rho_0^2$  refer to the maximal and the equilibrium values of the trace  $R_{\gamma\gamma}$ . Since in most applications  $\rho_m \gg \rho_0$  the Peterlin function can also be written approximately as  $P(r, t) \approx (1/(1 - \alpha R_{\gamma\gamma}))$  where  $\alpha = \rho_m^{-2}$ . In its turn the conformation tensor appears in the equations for fluid velocity  $u_\alpha(r, t)$  as an additional stress tensor:

$$\frac{\partial u_\alpha}{\partial t} + (u_\gamma \nabla_\gamma) u_\alpha = -\nabla_\alpha p + \nu_s \nabla^2 u_\alpha + \nabla_\gamma T_{\alpha\gamma} + F_\alpha , \quad (2.3)$$

$$T_{\alpha\beta}(r, t) = \frac{\nu_p}{\tau} \left[ \frac{P(r, t)}{\rho_0^2} R_{\alpha\beta}(r, t) - \delta_{\alpha\beta} \right] . \quad (2.4)$$

Here  $\nu_s$  is the viscosity of the neat fluid,  $F_\alpha$  is the forcing and  $\nu_p$  is a viscosity parameter which is related to the concentration of the polymer, i.e.  $\nu_p/\nu_s \sim c_p$  where  $c_p$  is the volume fraction of the polymer. We note however that the tensor field can be rescaled to get rid of the parameter  $\alpha$  in the Peterlin function,  $\tilde{R}_{\alpha\beta} = \alpha R_{\alpha\beta}$  with the only consequence of rescaling the parameter  $\nu_p$  accordingly. Thus the actual value of the concentration is open to calibration against the experimental data. Also, in most numerical simulations, the term  $P\rho_0^{-2}R$  is much larger than unity and the unity tensors in (2.1) and (2.4). Therefore, in the theoretical development below we shall use the approximation

$$T_{\alpha\beta} \sim \frac{\nu_p}{\tau} \frac{P}{\rho_0^2} R_{\alpha\beta} . \quad (2.5)$$

These equations were simulated on the computer in a channel or pipe geometry, reproducing the phenomenon of drag reduction in experiments. The most basic characteristic of the phenomenon is the increase of fluid throughput in the channel for the same pressure head, compared to the Newtonian flow. This phenomenon is demonstrated in Fig. 1 right taken from De Angelis et. al. (2003). As one can see the simulation is limited compared to experiments; the Reynolds number is relatively low, and the MDR is not attained. Nevertheless the phenomenon is there, and we will be able to use the simulation to asses and support the theoretical steps taken in the theoretical development. We should note that in the simulations one needs to add a small artificial viscosity to Eq. (2.1), in the form of a term  $\kappa \Delta R_{\alpha\beta}$ . This is done solely for taming numerical instabilities, and has very little consequence on the theory presented below, where it is not taken into account.

### 3. The derivation of the MDR

#### 3.1. Exact balance equations

Consider the fluid velocity  $U_\alpha(r)$  as a sum of its (time) average and a fluctuating part:

$$U_\alpha(r, t) = V_\alpha(y) + u_\alpha(r, t) , V_\alpha(y) \equiv \langle U_\alpha(r, t) \rangle . \quad (3.1)$$

For a channel of large length and width all the averages, and in particular  $V_\alpha(y) \rightarrow V(y)\delta_{\alpha y}$ , are functions of  $y$  only. The objects that enter the theory are the mean shear

$S(y)$ , the Reynolds stress  $W(y)$ , the kinetic energy  $K(y)$  and the mean conformation tensor  $\langle R(y) \rangle$ ; the first three are defined respectively as

$$S(y) \equiv dV(y)/dy, \quad W(y) \equiv -\langle u_x u_y \rangle, \quad K(y) = \langle |u|^2 \rangle / 2.$$

Taking the long time average of Eq. (2.3), and integrating the resulting equation along the  $y$  coordinate produces an exact equation for the momentum balance:

$$W + \nu S + \frac{\nu_p}{\tau} \langle PR_{xy} \rangle (y) = p'(L - y). \quad (3.2)$$

where  $p'$  is the pressure gradient and  $L$  is the mid-channel height. The RHS is simply the rate at which momentum is produced by the pressure head, and on the LHS we have the Reynolds stress which is the momentum flux, the viscous dissipation of momentum, and the rate at which momentum is transferred to the polymers. Near the wall it is permissible to neglect the term  $p'y$  on the RHS for  $y \ll L$ . Next we want to derive the balance equation for energy. To this aim we need to take into account the extra energy dissipation due to transfer of energy from the velocity field to the polymers. This energy dissipation, denoted as  $\epsilon_p$ , in the limit of validity of (2.5) can be exactly computed to be

$$\epsilon_p = \frac{\nu_p}{2\tau^2} \langle P^2 \text{Tr} R_{\alpha\beta} \rangle, \quad (3.3)$$

where  $\text{Tr} R_{\alpha\beta} \equiv R_{xx} + R_{yy} + R_{zz}$ . As stated in Eq. (3.1), we split the velocity field into its mean and the fluctuation, and consider separately the balance equation for the mean energy  $V^2$  and for the turbulent energy  $\langle u^2 \rangle$ . The former yields an equation identical to (3.2) but multiplied by  $S$ :

$$WS + \nu S^2 + \frac{\nu_p}{\tau} \langle PR_{xy} \rangle (y) S = p'LS. \quad (3.4)$$

On the other hand the balance equation for the turbulent energy cannot be written exactly. To understand how to write it, we need to identify first the meaning of the third term on the LHS of Eq. (3.4). To gain insight on how to represent properly this term we consider how to estimate correlations containing the tensor  $R_{ij}$ . Using equation (2.1), we obtain on the average:

$$\frac{\partial}{\partial y} \langle u_y R_{ij} \rangle = -\frac{1}{\tau} \langle PR_{ij} \rangle + \langle R_{ik} \partial_k u_j \rangle + \langle R_{jk} \partial_k u_i \rangle. \quad (3.5)$$

### 3.2. Closure approximations

To proceed, we employ a 1-point closure approximation, keeping only terms that survive this closure. In this approximation, the only terms  $\langle \partial_k u_j R_{ik} \rangle$  which survive are proportional to  $S$ , i.e.

$$\langle R_{ik} \partial_k u_j \rangle = a_i S \langle R_{ij} \rangle \delta_{jx} \quad (3.6)$$

where  $a_i$  are constant of order 1. For  $i = x, y$ , using (3.6), equations (3.5) give:

$$\frac{1}{\tau} \langle P \rangle \langle R_{xx} \rangle = 2a_x \langle R_{xy} \rangle S, \quad (3.7)$$

$$\frac{1}{\tau} \langle P \rangle \langle R_{xy} \rangle = a_y \langle R_{yy} \rangle S. \quad (3.8)$$

To test the quality of this closure we check each term by DNS, comparing between the exact and approximated forms. A description of the DNS simulations is reported in De Angelis et. al. (2003).

In Figs. (2) we show the comparison of the 1-point closure approximation, using numerical simulations with  $a_x = 1$  and  $a_y = 0.45$ . The overall comparison is reasonably

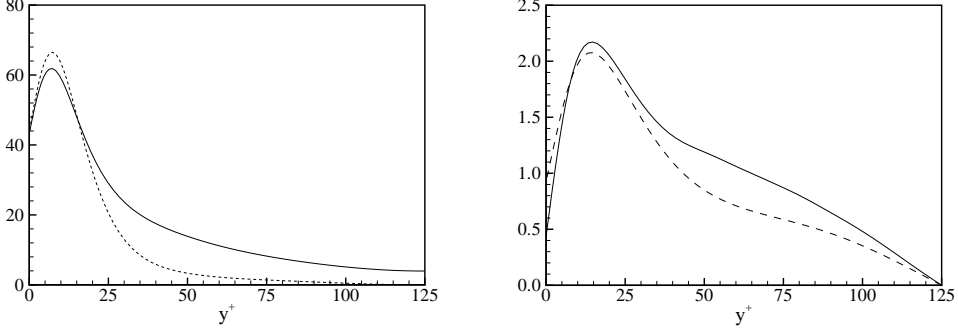


FIGURE 2. Left panel: quality of the 1-point closure for equation (3.7) as obtained by direct numerical simulation for a turbulent channel flow, see De Angelis et. al. (2003). The continuous line refers to the term  $2a_x R_{xy} S$  with  $a_x = 1$  while the dashed line to the term  $\langle P \rangle \langle R_{xx} \rangle / \tau$ . The two terms are of the same order of magnitude within the buffer region. Right panel: comparison of the 1-point closure approximation for equation (3.8). The continuous line refers to the term  $a_y R_{yy} S$  with  $a_y = 0.45$ , while the dashed line to the term  $\langle P \rangle \langle R_{xy} \rangle / \tau$ . The two terms are of the same order of magnitude within the buffer region.

good within the buffer layer, i.e. in the region where the polymers enhance the mean flow with respect to the Newtonian case. We can thus safely proceed and learn from Eq. (3.7) that in 1-point closure we can write the third term on the LHS of Eq. (3.4) as

$$\frac{\nu_p}{\tau} \langle P R_{xy} \rangle (y) S = \frac{\nu_p}{2\tau^2} \langle P \rangle^2 \langle R_{xx} \rangle ; \quad (3.9)$$

as such, it is one of the three terms appearing in the trace in Eq. (3.3). As this term is already exhausted in the balance for the mean energy  $V^2$ , this leaves for the turbulent energy balance equation the other two terms. We stress here that this conclusion rests entirely on the numerical value  $a_x = 1$ . We propose that this is essentially exact, even though at this stage we present it on the basis of numerical comparisons. In future work we will derive this important fact from first principles.

We can therefore write now the balance equation for the turbulent energy. The rate of production is simply  $W(y)S(y)$ . This production of energy is balanced by the energy dissipation  $\nu \langle |\nabla u|^2 \rangle$  and the two terms in the energy transferred to the polymer (3.3). The energy dissipation is estimated differently in the viscous layer near the wall and in the bulk of the turbulent flow, namely

$$a\nu \frac{K}{y^2} + b \frac{K^{3/2}}{y} + \frac{A^2 \nu_p}{2\tau^2} \langle P \rangle^2 (\langle R_{yy} \rangle + \langle R_{zz} \rangle) = WS , \quad (3.10)$$

where the first term reflects the smoothness of the field in the viscous layer, and the second term is a standard Kolmogorov-type estimate of the energy flux as the typical energy at distance  $y$  from the wall over the typical eddy turn-over time  $y/\sqrt{K(y)}$ . These estimates are identical to the Newtonian case. The new (and somewhat difficult) term is the third term on the LHS, where  $A$  is a constant to be computed.

To evaluate this last term, we refer again to our DNS results to assess the relative importance of  $\langle R_{yy} \rangle$  and  $\langle R_{zz} \rangle$ : these objects are very close to each other throughout the region of concern in the channel. We therefore can keep only one of them by redefining consequently the constant  $A$ :

$$a^2 \nu \frac{K}{y^2} + b \frac{K^{3/2}}{y} + \frac{A^2 \nu_p}{2\tau^2} \langle P \rangle^2 \langle R_{yy} \rangle = WS . \quad (3.11)$$

### 3.3. Reminder: the von-Kármán law

At this point it is useful to remind to the reader the derivation of the von-Kármán log law of the wall in the Newtonian case, see Pope (2000). The terms including the conformation tensor in Eqs. (3.2) and (3.11) are not present in this case. Outside the boundary layer the viscous terms proportional to  $\nu$  are neglected, and we therefore get from Eq. (3.2) the result that  $W$  is constant,  $W \approx p'L$ , and from Eq.(3.11) that  $bK^{3/2}/y \sim WS$ . Now one introduces the experimental knowledge that  $K$  and  $W$  are proportional to each other outside the viscous boundary layer:

$$W = c_N^2 K . \quad (3.12)$$

This equation can be presented as a rigorous inequality  $W \leq K$  (i.e.  $c_N$  is at most unity), and it can be justified phenomenologically as a result of the scale invariance. We will take it, and its visco-elastic counterpart

$$W = c_V^2 K , \quad (3.13)$$

as given experimental inputs. Using (3.12) in the relations obtained for the Newtonian case, we find immediately  $S \propto \sqrt{p'L}/y$  which integrates to the log-law of the wall  $V = \log y/\kappa_K + B$  where the von-Kármán constant  $\kappa_K$  and the intercept  $B$  are phenomenological constants.

### 3.4. Derivation of the MDR

We anticipate that in the viscoelastic case the dominant terms in the balance equations (3.2) and (3.11) will be the terms including the polymer conformation tensor. To see that this is indeed the case, we analyze the  $yy$  component of Eq. (3.5). It reads

$$\frac{\partial}{\partial y} \langle u_y R_{yy} \rangle = -\frac{1}{\tau} \langle P R_{yy} \rangle + 2 \langle R_{yk} \partial_k u_y \rangle . \quad (3.14)$$

In 1-point closure this equation gives the absurd result  $\langle P R_{yy} \rangle = 0$  which means that in this case we must proceed to the next order and estimate

$$\langle R_{yk} \partial_k u_y \rangle \approx \langle R_{yy} \rangle [K(y)/y^2]^{1/2} \approx c_V \langle R_{yy} \rangle [W(y)/y^2]^{1/2} . \quad (3.15)$$

Using this estimate we can proceed to conclude from Eq. (3.14) that

$$\frac{1}{\tau} \langle P \rangle \langle R_{yy} \rangle = g \langle R_{yy} \rangle W^{1/2}(y)/y , \quad (3.16)$$

where  $g$  is an empirical constant. Because equation (3.16) is crucial for the evaluation of the momentum flux in the buffer layer, we show in Fig. 3 (left panel) the quality of the closure approximation as obtained by numerical simulations. As one can see, the quality of the approximation is rather good within the buffer layer.

This allows us to offer a final result for  $W(y)$  in which the polymer conformation tensor disappears altogether:

$$W(y) \sim \frac{\langle P \rangle^2 y^2}{g^2 \tau^2} . \quad (3.17)$$

This is an important result. On the one hand it shows how the Reynolds stress is reduced in the elastic layer, providing a direct mechanism to drag reduction. The Reynolds stress is the momentum transfer to the wall, and reducing it results in an increase of the mean momentum, in order to balance the constant rate of momentum production  $p'L$ . On the other hand, we see that this quantity is becoming of  $O(y^2)$ , justifying the neglect of

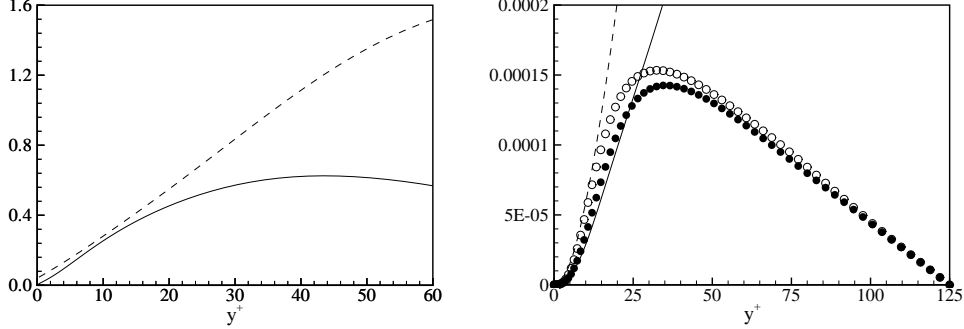


FIGURE 3. Left panel: Comparison between the term  $\langle R_{yy} \rangle \langle P \rangle / \tau$  and  $\langle R_{yy} \rangle W^{1/2} / y$  in the numerical simulations. Right panel: Comparison of  $W$  as obtained by direct numerical simulations against the theoretical estimate  $y^2 \langle P \rangle^2 / \tau^2$  for two different values of  $\tau$ , namely  $\tau = 12.5$  and  $\tau = 37.5$ . The estimate of  $g$  for the two cases gives  $g = 1.22$  for  $\tau = 12.5$  and  $g = 1.1$  for  $\tau = 37.5$ . Thus, although the value of  $\tau$  changes by a factor 9, the combination of the Peterlin function with the  $\tau^{-2}$  term gives the same overall constant within 10 *per cent* error, showing the excellent quality of the prediction (3.17)

Reynolds stresses in the simplified theory of L'vov et. al. (2003). In Fig. 3 (right panel) we compare the prediction of equation (3.17) against the direct numerical simulations. The quality of the results are extremely good, showing that the right physical behavior has been captured by employing the closure approximations.

Neglecting then the first two terms in eq. (3.2), without the term  $p'y$ , and eq (3.11), and using the result (3.8) for the conformation tensor we end up with the estimate for the shear  $S(y)$  in the form

$$S \sim \frac{Ag}{\sqrt{2a_y}} \frac{\sqrt{p'L}}{y}. \quad (3.18)$$

Let us note that (3.18) is independent of  $\tau$  and it is consistent with the findings of L'vov et. al. (2003), i.e. it predicts a new logarithmic law of the wall which is the MDR asymptote. We note that the dissipative terms did not play any role in the viscoelastic derivation; the polymer terms took over, providing precisely the same role of the effective viscosity introduced in the simplified theory of L'vov et. al. (2003).

In order to compute the value of  $A$ , we invoke the estimate of  $a$  in equation (3.11) as obtained in L'vov et. al. (2003), i.e.  $a = y_v^+ c_N$  where  $y_v^+$  is the thickness of the viscous sub-layer, for the Newtonian fluid, expressed in the Prandtl units  $y^+ \equiv y\sqrt{p'L}/\nu$ . Next, we compute the value of  $y_F$  for which the MDR mean flow shear is equal to the viscous mean flow shear:

$$\frac{Ag}{\sqrt{2a_y}} \frac{\sqrt{p'L}}{y_F} = \frac{p'L}{\nu},$$

which gives, in Prandtl units,

$$y_F^+ = \frac{Ag}{\sqrt{2a_y}}. \quad (3.19)$$

For  $y = y_F$  we expect that the energy dissipation due to viscous effect  $a\nu K/y_F^2$  is of the order of the energy dissipation due to polymers stretching, i.e.

$$a^2 \nu \frac{K}{y_F^2} \sim \frac{A^2 \nu_p}{2\tau^2} \langle P \rangle^2 \langle R_{yy} \rangle.$$

Finally, by using the MDR estimate (3.18) and equations (3.8), (3.17), and (3.19), we can compute the value of  $A$ . It turns out that for the MDR slope  $Ag/\sqrt{2a_y} \sim y_v^+(c_N/c_V)$ , in agreement with the previous findings of L'vov et. al. (2003).

#### 4. Saturation of drag reduction and cross over from the MDR to the Newtonian plug

We expect a cross over from the MDR asymptote back to the Newtonian plug when the basic assumptions on the relative importance of the various terms in the balance equations lose their validity. Experimentally one sees that mean velocity profile follows the MDR up to some point  $y_V^+$  after which it crosses over back to a logarithmic profile with the same slope as the Newtonian flow. To measure the quality of drag reduction one can introduce a dimensionless drag reduction parameter

$$Q \equiv \frac{y_V^+}{y_N^+} - 1. \quad (4.1)$$

The Newtonian flow is then a limiting case of the viscoelastic flow corresponding to  $Q = 0$ . There can be a number of reasons for the saturation of the drag reduction effect. One reason that can be important for large Reynolds numbers is that the concentration of the polymer is too small to provide the necessary increase in the effective viscosity as a function of the  $y^+$ . This mechanism for the cross over back to the Newtonian plug was discussed in full detail in Benzi et. al. (2004). The main result of Benzi et. al. (2004) is that the drag reduction parameter  $Q$  is given by

$$Q = \alpha^3 c_p N_p^3 \quad c_p \text{ small, } Re \text{ large,} \quad (4.2)$$

where  $c_p$  is the number density (concentration in number of molecules per unit volume) of the polymer and  $N_p$  is the degree of polymerization (the number of monomers per molecule). The parameter  $\alpha$  is the linear scale of the monomer. This prediction was tested in Benzi et. al. (2004) by comparing with experiments with DNA as the drag reducing agent, with excellent agreement between theory and experiments.

Here we address another mechanism for the saturation of drag reduction. We expect a cross over from the MDR asymptote back to the Newtonian plug when the basic assumptions on the relative importance of the various terms in the balance equations lose their validity, i.e. when (i) the turbulent momentum flux  $W$  becomes comparable to the total momentum flux  $p'L$ , or when (ii) the turbulent energy flux  $bK^{3/2}/y$  becomes of the same order as the turbulent energy production  $WS$ . Using the estimates (3.17) and (3.18), one finds that both these conditions give the same cross-over point

$$y_V \simeq \frac{\tau \sqrt{p'L}}{\langle P \rangle g}. \quad (4.3)$$

Note that  $\tilde{\tau}(y) \equiv \tau / \langle P(y) \rangle$  is the effective non-linear polymer relaxation time. Therefore Eq. (4.3) can be also rewritten as

$$S(y_V) \tilde{\tau}(y_V) \simeq 1. \quad (4.4)$$

In writing this equation we use the fact that the cross over point belongs also to the edge of the Newtonian plug where  $S(y) \approx \sqrt{p'L}/y$  and that  $g \sim 1$ . The LHS of this equation is simply the *local Weissenberg number* (product of local mean shear and local effective polymer relaxation time). Thus, *the cross-over to the Newtonian plug occurs at the point, where the local Weissenberg number decreases to  $\sim 1$* . We expect that this result remains



valid for any model of the elastic polymers, not only for the FENE-P model considered here.

To understand how the cross-over point  $y_V$  depends on the polymer concentration and other parameters, we need to estimate mean value of the Peterlin function  $\langle P \rangle$ . Let us estimate the value of  $\langle P \rangle$  as

$$\langle P \rangle = \frac{1}{1 - \alpha \langle R \rangle},$$

where  $\langle R \rangle = \langle R_{xx} + R_{yy} + R_{zz} \rangle \sim \langle R_{xx} + 2R_{yy} \rangle$  and  $\alpha \sim 1/\rho_m^2$  (for simplicity we disregard  $\rho_0$ ). It follows from Eqs. (3.7)-(3.8), that

$$\langle R_{xx} \rangle \simeq (S\tilde{\tau})^2 \langle R_{yy} \rangle,$$

and at the cross-over point (4.4)

$$\langle R_{xx} \rangle \simeq \langle R_{yy} \rangle, \quad \langle R \rangle \simeq \langle R_{yy} \rangle.$$

The dependence of  $\langle R_{yy} \rangle$  on  $y$  in the MDR region follows from Eqs. (3.11), (3.17), and (3.18):

$$\langle R_{yy} \rangle \simeq \frac{\tilde{\tau}^2 W S}{\nu_p} \simeq \frac{y \sqrt{p' L}}{\nu_p}.$$

Then at the cross-over point  $y = y_V$ :

$$\langle P \rangle \simeq \frac{1}{1 - \alpha y_V \sqrt{p' L} / \nu_p}.$$

Substituting this estimation into (4.3) gives the final result

$$y_V = \frac{C \tau \sqrt{p' L}}{1 + \alpha p' L \tau / \nu_p}. \quad (4.5)$$

Here  $C$  is constant of the order of unity. Finally, introducing the dimensionless concentration of the polymers

$$\tilde{c}_p \equiv \frac{\nu_p}{\alpha \nu_0}, \quad (4.6)$$

we write the denominator in Eq. (4.5) as

$$1 + \frac{\alpha p' L \tau}{\nu_p} = 1 + \frac{1}{\tilde{c}_p} \frac{p' L \tau}{\nu_0} = 1 + \frac{\text{We}}{\tilde{c}_p}.$$

Here

$$\text{We} \equiv \frac{p' L \tau}{\nu_0} \quad (4.7)$$

is the (global) Weissenberg number. The final result for the dimensionless cross-over point  $y_V^+ \equiv y_V \sqrt{p' L} / \nu_0$  assumes a very simple form:

$$y_V^+ = \frac{C \text{We}}{1 + \text{We} / \tilde{c}_p}. \quad (4.8)$$

This prediction can be put to direct test when  $\tilde{c}_p$  is very large, or equivalently in the Oldroyd B model where  $P \equiv 1$  Benzi et. al. (2004). Indeed, in numerical simulations when the Weissenberg number was changed systematically, cf. Yu et. al. (2001), one observes the cross over to depend on We in a manner consistent with Eq. (4.8). The other limit when  $\tilde{c}_p$  is very small is in agreement with the linear dependence on  $\tilde{c}_p$  predicted in Eq. (4.2).

We can thus reach conclusions about the saturation of drag reduction in various limits of the experimental conditions, in agreement with experiments and simulations.

## 5. Conclusions

In this paper we showed how to understand some of the most common effects of dilute polymer solutions in wall bounded turbulent flows. Our starting point is the FENE-P model which has been shown to provide good qualitative and quantitative agreement with experimental findings. Within the context of the FENE-P model, we were able to derive in a controlled way the universal MDR profile that was first obtained theoretically in L'vov et. al. (2003). One of our main predictions is provided by Eq. (3.17) which tells us how the Reynolds stress behaves as a function of the Peterlin function and the polymer relaxation time  $\tau$ . The predictions are in very good agreement with the results of DNS. In particular, Eq. (3.17) shows that the Reynolds stress is proportional to  $\langle P \rangle^2 \tau^{-2}$ , i.e. it becomes small for long polymer chains ( $\tau$  large) and large concentration. The velocity profile comes out independent on the concentration up to a point,  $y_V^+$ , given by Eq. (4.8), where the von-Kármán law is restored. In general our theoretical approach rationalizes and predicts a large number of qualitative and quantitative aspects of drag reduction as seen in laboratory experiments and in DNS of the FENE-P model.

This work was supported in part by the European Commission under a TMR grant, the US-Israel Binational Science Foundation, and the Minerva Foundation, Munich, Germany.

## REFERENCES

- LUMLEY J.L. 1969 *Ann. Rev. Fluid Mech.* **1**, 367.  
 SREENIVASAN K.R. WHITE C.M. 2000 *J. Fluid Mech.* **409**, 149.  
 VIRK P.S. 1969 *J. AIChE* **21**, 625.  
 DE ANGELIS E., C.M. CASCIOLA, V.S. L'VOV, R. PIVA AND I. PROCACCIA 2003 *Phys. Rev. E.* **67**, 056312 .  
 WARHOLIC M.D., H.MASSAH, T.J. HANRATTY 1999 *Experiments in Fluids*, **27**, 461.  
 ROLLIN A.,F.A. SEYER 1972 *Can. J. Chem. Eng.***50**, 714-718.  
 L'VOV V.S., A. POMYALOV, I. PROCACCIA, V. TIBERKEVICH 2003 *Phys. Rev. Lett.* submitted, also: nlin.CD/0307034.  
 RUDD M.J., 1969 *Nature*, **224**, 587.  
 DE ANGELIS E., C. CASCIOLA, V. S. L'VOV, A. POMYALOV, I. PROCACCIA, V. TIBERKEVICH 2004 Drag Reduction by a linear viscosity profile, *Phys. Rev. E*, submitted, also: nlin.CD/0401005  
 BIRD R.B., C.F. CURTISS, R.C. ARMSTRONG, O. HASSAGER, 1987 *Dynamics of Polymeric Fluids Vol.2* (Wiley, NY).  
 BERIS A.N., B.J. EDWARDS 1994, *Thermodynamics of Flowing Systems with Internal Microstructure* (Oxford University Press, NY).  
 POPE S.C., 2000 *Turbulent Flows* (Cambridge).  
 BENZI R., V. S. L'VOV, I. PROCACCIA V. TIBERKEVICH , 2004 *Saturation of Turbulent Drag Reduction in Dilute Polymer Solutions* *Phys. Rev. Lett* in press, Also:nlin.CD/0402027  
 BENZI R., E. CHING, N. HORESH, I. PROCACCIA, 2004, Theory of concentration dependence in drag reduction by polymers and of the MDR asymptote, *Phys. Rev. Lett. Feb* **20** .  
 YU B., Y. KAWAGUCHI, S TAKAGI, Y. MATSUMOTO 2001, The 7th symposium on smart control of turbulence, University of Tokyo.